What's all that noise? An Investigation of the Faint Radio Properties of Quasars

Lauren Fossel, Williams College and Ché Bradley, Middlebury College

Advisor: Eilat Glikman, Middlebury College

Abstract

We investigate the radio properties of quasars and strong quasar candidates by data mining and analyzing the deep VLA observations in Stripe 82. Previous research found that radio emission in quasars appears bimodal: they are either "radio loud" or "radio quiet", but newer data refute this claim. This analysis probes deeper in both the radio and optical data, and provides evidence against a radio bimodality. We use image stacking of quasar sub-samples to determine their median radio properties and investigate the relationship between redshift, optical luminosity, and radio loudness. Furthermore, we categorize the radio-detected quasars by morphology to explore morphological differences between optically luminous and optically dim quasars. Finally, we analyze and compare the radio properties of blue versus red quasars by stacking their radio images. We show that the average red quasar is more radio luminous than the average blue quasar, a result that requires further exploration.

Introduction

Quasars are supermassive black holes at the centers of galaxies into which gaseous material falls. This material shines brightly, which enables astronomers to study black holes during their period of active growth. Although quasars were initially discovered at radio wavelengths, only about 10% of sources emit strong radio waves. Furthermore, a larger fraction of red quasars seem to emit strong radio waves (Klindt et al. 2019), a claim which our own data support. The origin of the radio emission in quasars remains a mystery, but previous research claims there exists a bimodality between radio loud and radio quiet quasars (Ivezić et al. 2002). Kratzer et al. (2015) explains how going deeper into the radio while neglecting the optical creates a selection bias that would artificially suggest a bimodal distribution.

The Data

We perform our work in a region of sky called Stripe 82 that covers 270 deg^2 and has been imaged extensively at many wavelengths and co-added to produce a deep optical image (Jürgen Fliri et al. 2016). Overlapping this region are 100 deg^2 of deep radio observations with the Very Large Array (VLA) that we focus on in this work. This radio data probes three times deeper in the radio than the previous FIRST survey (which also overlaps this region), allowing us to uncover fainter objects.

We implemented the following steps to study the radio properties of quasars in this region:

- We matched the quasars that had VLA radio detections to the deep optical co-added data in the 100 deg^2 region of Stripe 82.

- We then matched that file to confirmed quasars from all available catalogs at all wavelengths. The vast majority of quasars came from the SDSS Quasar Catalog and the Milliquas Catalog version 6.3. After removing any duplicates or objects without a redshift, we achieved a sample of 683 quasars.

- To help strengthen our sample we also included a sample of strong quasar candidates. We followed the procedures Kratzner et al (2015) used to create their analogous sample of strong quasar candidates with photometric redshifts (which are less reliable than spectroscopic redshifts). We found 16 strong quasar candidates that also had matches in the deep VLA radio observations, for a total of 699 quasars with radio and optical detections.

Radio is a measure of the quasar's emission at a wavelength of 20 cm and the optical is measured at a red wavelength called the "i-band" (7625 Å, just beyond what the human eye can detect). Radio loudness, parametrized by R, represents the ratio of radio emission (flux) to optical emission (flux) in quasars. However, astronomers use magnitudes which are on a logarithmic scale:

$$magnitude = -2.5log\frac{flux}{3631Jy} \tag{1}$$

where Jy is a Jansky, and 1 Jy = 10^{-26} W/m^2/Hz. A ratio is actually a difference in log space, so

$$R = 0.5(i - t) \tag{2}$$

In Figure 1, total integrated radio flux was converted to a radio magnitude, t, using the equation from Ivezić et al. (2002):

$$t = -2.5log\frac{F_{int}}{3631Jy} \tag{3}$$

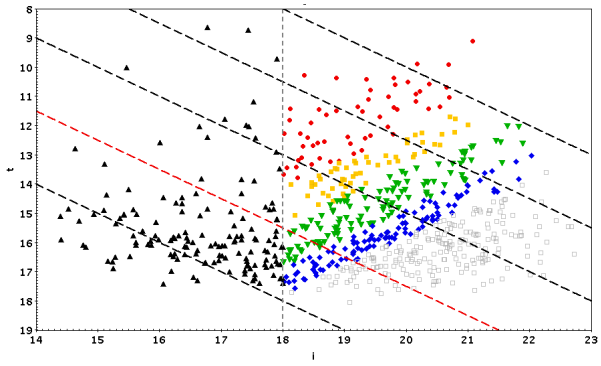

Fig. 1.— This plot shows the radio magnitude (t = -2.5 log($\frac{f_{radio}}{3631Jy}$)) of 699 deep VLA stripe 82 confirmed quasars and strong quasar candidates as a function of optical magnitude (i = -2.5 log($\frac{f_{radio}}{3631Jy}$)). The diagonal dashed lines show the lines of constant R values, from R=0 to R=4 . Objects close to the upper right hand corner are the most radio loud. The vertical dashed line shows the i=18 cutoff. Points are shown with different shapes to represent the strips perpendicular to the lines of constant R values. The objects represented by the open grey squares were not included in our analysis because they are on the edge of the detection limits.

The detection limits of the surveys in both the radio and optical frequencies have a direct effect on the distribution of radio loudness, R. We followed Ivezić et al. (2002) in creating strips perpendicular to the constant R lines that are not affected by the magnitude detection limits in order to reduce selection bias. We then analyzed the distribution of R values within those strips.

Figure 1 shows the range of radio and optical magnitudes for all the quasars with detections in the VLA survey in our area of study. There were a total of 16,663 quasars in the region of interest, but only the 699 in Figure 1 were bright enough in the radio to be detected in the deep VLA survey.

Radio Bi-Modality

Previously when a plot of R distributions was made using FIRST data (as in Ivezić et al. (2002), displayed in Figure 2) before the deep VLA stripe 82 detections existed, the plot showed a dip in quantity of objects around R = 1 to R = 2.5, leading to the idea that there is a quasar radio bimodality. However, those data were strongly limited by the depth of i and t. As seen in Figure 3, when deeper data are added, the dip is filled in by objects of "intermediate" radio loudness. This suggests that the apparent radio bi-modality was merely due to selection bias.

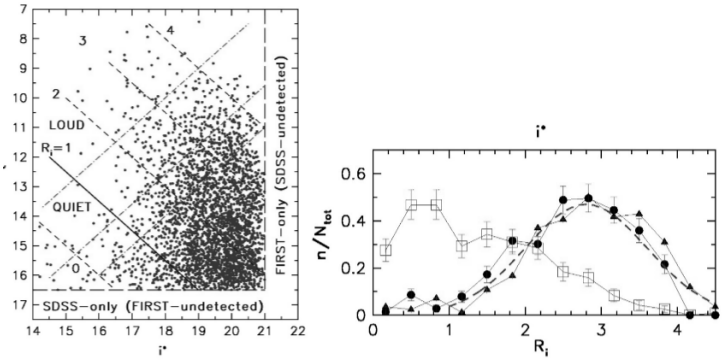

Fig. 2.— Plots from Ivezić et al (2002). The left and right plots are analogous to our Figure 1 and Figure 3 respectively, but use shallower radio data from the FIRST survey. The rightmost plot shows the apparent radio bimodality, which our data suggests is merely due to selection effects.

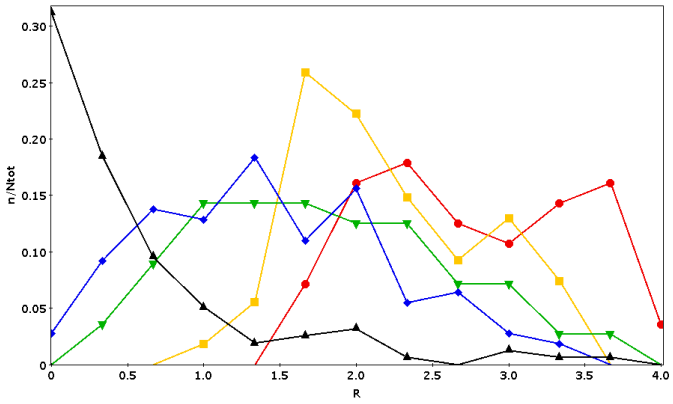

Fig. 3.— The normalized distribution of R values for each strip shown in Figure 1. This data, which probes deeper in both the optical and radio wavelengths, resolves FIRST's bias and erases the bimodality.

Stacking

Stacking shows how quasars that may be undetected by radio telescopes still emit radio waves. A quasar detected at optical wavelengths will have its exact position recorded, so when we enter that location into a survey of the radio sky, we know it will be at the center of the image. With this in mind, we can take many images of undetected quasars and essentially place them on top of each other. Since we treat an image as a 2-dimensional grid of pixels, stacking them will align all the pixels at any given point along the third dimension. Every pixel has a value that corresponds to the flux at that point, so every column becomes a list of values. With many images, taking the median value of the columns causes the random background noise to approach zero. But for the quasars in the center, their median value would be higher than random noise, and so we see a brighter point in the center.

The radio images in Figure 4 show the value of stacking. The left and middle images both show quasars that have the same optical brightness, but clearly very different radio brightnesses. The left is strongly detected, with a radio flux of 168.44 mJy, whereas the middle figure is fainter than the background noise limit of 1 mJy. However, when we stacked 222 images similar to the middle image, we obtain the rightmost image. This image shows that when many radio quiet images are stacked, a source emerges from the background noise that is clearly visible and represents the average radio brightness of the 222 quasars (in this case, $2.33*10^{-5}$ mJy).

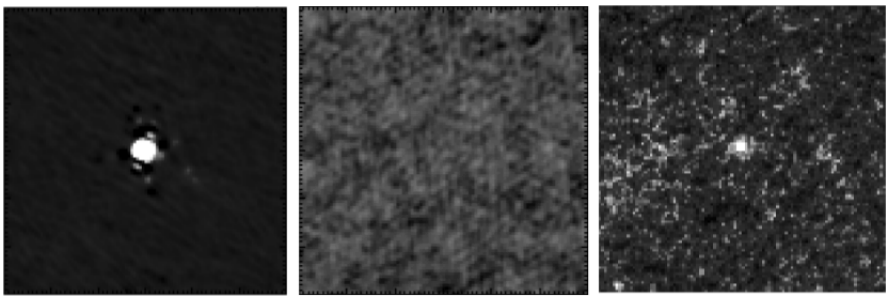

Fig. 4.— Left: A detected, radio loud quasar. Middle: A non-detected, radio quiet quasar. Right: A median stacked image of 222 radio quiet, non-detected quasars.

Red Versus Blue Quasars

The majority of known quasars have blue optical light resulting from the accretion of surrounding hot gas, but some quasars appear optically red. The apparent redness is likely a result of scattering of the blue light off of dust particles along the line of sight - an effect known as "dust-reddening" - but could also come from starlight contamination, excess flux at longer wavelengths, or differences in the accretion disc (Klindt et al. 2019). Red quasars are commonly found in recently merged galaxies, which are a likely source of the dust (Glikman et al. 2015).

We stacked images of quasars from both the FIRST and deep VLA surveys, concentrating on a sample from Glikman et al. (2018) in which blue and red quasars were uniformly selected by their infrared colors. The deep VLA survey only covers a thin band of sky, so there were fewer images in that sample. The samples consisted of 21 red quasars and 56 blue quasars from the FIRST survey, and 10 red quasars and 25 blue quasars from the deep VLA survey. The results of the stacking

process are presented below. They show that the red quasars (left) are more radio luminous than blue quasars (right) on average.

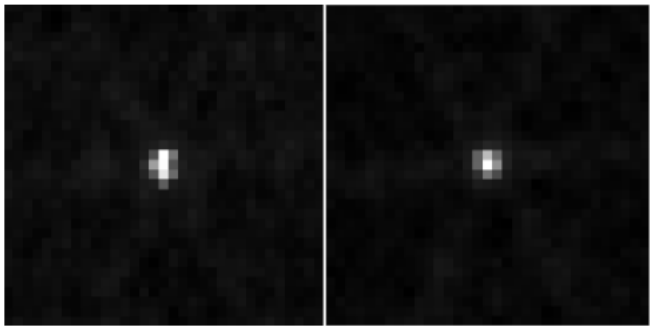

Fig. 5.— Left: stacked red quasars from FIRST. Right: stacked blue quasars from FIRST

Table 1: Results of stacking red and blue quasars from the deep VLA and FIRST

Survey	Red Flux (μJy)	Blue Flux (μJy)
Deep VLA	26.580 +/- 0.002	9.798 +/- 0.006
FIRST	7.87 +/- 0.02	5.64 +/- 0.01

But why would red quasars be more radio luminous than blue quasars? One theory suggests that the host galaxies of red quasars are involved in star formation, which is a process that produces radio waves. Since galaxy mergers are accompanied by an increase in star formation, this is consistent with what we might expect for these sources. To test this, we quantitatively compared the amount of radio emission between red and blue quasars, hoping the results might hint at underlying physical explanations. We found the median redshift for our two quasar samples to perform the calculation.

$$L = flux \cdot 4\pi \cdot d_{\mathrm{L}}(z)^2 \tag{4}$$

$$\nu Ldiff = 2.5 \cdot 10^{37} \psi erg^{-1} \tag{5}$$

where $\nu = 1.4 \cdot 10^9 Hz$, $\mathrm{d_L(z)^2}$ is the luminosity distance at a given redshift, and ψ is the rate of star formation. Our red and blue samples had median redshifts of 0.608 and 0.213 respectively. Then, using the above equations and solving for ψ, we have Lred = $4.092 \cdot 10^{29}$ erg $\mathrm{s^{-1}}$ $\mathrm{Hz^{-1}}$ and Lblue = $1.297 \cdot 10^{28}$ erg $\mathrm{s^{-1}}$ $\mathrm{Hz^{-1}}$. This means Ldiff = $3.962 \cdot 10^{29}$ erg $\mathrm{s^{-1}}$ $\mathrm{Hz^{-1}}$ and
$\psi = \frac{(1.4 \cdot 10^9 Hz)(3.962 \cdot 10^{29} erg\ s^{-1}\ Hz^{-1})}{2.5 \cdot 10^{37} erg\ s^{-1}} \approx 22 \frac{M_\odot}{yr}$
This is a reasonable rate for star formation in these quasars, which suggests it may be the cause for the observed excess radio emission.

Typical Radio Loudness Based on Red-Shift and Optical Luminosity

The next step in understanding radio emission of quasars is analyzing the radio loudness of quasars based on redshift and optical luminosity. We used the 16,663 quasars located in the area of Stripe 82 that the deep VLA observations were taken in and plotted them based on redshift and optical luminosity. The majority of these objects were too radio faint to be detected by the deep

VLA observations in Stripe 82. Though they had no significant radio detection, it is possible to learn something about the radio properties of these objects by stacking their images to measure their average radio properties.

We split the luminosity-redshift space into 75 boxes, each with 222 objects. For every object within each box, we downloaded its radio image and performed a median stacking procedure to determine the average radio brightness for objects within the specified luminosity and redshift range. This then allowed us to determine the median R value within each box, and from that, how R relates to optical luminosity and redshift. The results of these procedures are depicted in Figure 6.

The left side of Figure 6 shows the average radio loudness of the typical quasar at a particular redshift and luminosity range. From the figure, it can be seen that the highest luminosity quasars are quieter in the radio than the lower luminosity quasars. There is no strong trend with redshift, except for the lowest redshift objects seem to be particularly radio quiet. This could be explained by the fact that the early universe seems to have been much more active than it is now. This means that at the closest redshifts we would expect to see a decline in brightness and number of quasars.

Kratzer et al. (2015) did a similar boxing and stacking procedure, but looked at the radio loud fraction (the fraction of radio loud quasars, R>1). They found that the radio loud fraction increases with optical luminosity, as seen on the right side of Figure 6. Because Kratzer's analysis used a mean, their results are more affected by strong, bright outliers. By using the median, our analysis looks at the typical quasar, and shows that the trend of the median does not follow the trend of the radio loud fraction from Kratzer. This means that our data suggests that the typical optically dim quasar is more radio loud than the typical optically bright quasar (though in both cases R is well below the radio loud threshold R=1), and that the increase in the radio loud fraction with optical luminosity is likely due to bright jet outliers. This suggests that a different radio-producing physics is at play in the typical quasar, such as star formation or possibly a shocked wind (Faucher-Gugiere et al. 2012).

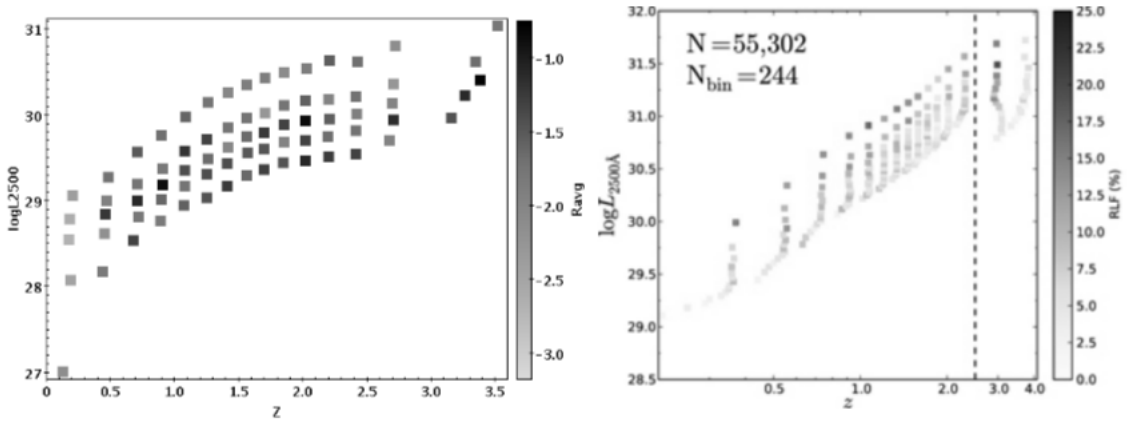

Fig. 6.— Left: Average R values for objects grouped by redshift and optical luminosity. Each square represents 222 objects in that region of red-shift and optical luminosity. Right: Plot from Kratzer et al. (2015) showing the radio loud fraction for points in redshift-luminosity space.

Morphology

To explore the role of jets in the radio emission of quasars, we investigated whether there are morphological differences in quasars based on radio loudness. We extracted two subsets from the objects represented in the left side of Figure 6: the objects with the highest optical luminosity for each vertical strip, and the objects with the second lowest luminosity for each vertical strip. We chose to use the objects with the second lowest rather than the lowest luminosity, since some of the lowest luminosity objects may be missing because they are on the threshold of the detection limit. We then downloaded the radio images for the objects in these subsets that were detected by the VLA observations. We categorized each object as belonging to one of four categories based on the classes used by Klindt et al. (2019):

- **Faint** objects detected near the VLA detection threshold with peak fluxes of Fpeak < .78 mJy.
- **Compact** objects that are point-like with no extended emission, and have Fpeak > .78 mJy.
- **Extended** single radio sources that are extended. If these sources have lobes, the lobes are fainter than the quasar core.
- **FR II-like** Double lobed sources with similar brightnesses and offsets from the quasar. At least one lobe is brighter than the quasar core.

The results of these classifications are shown in Figure 7.

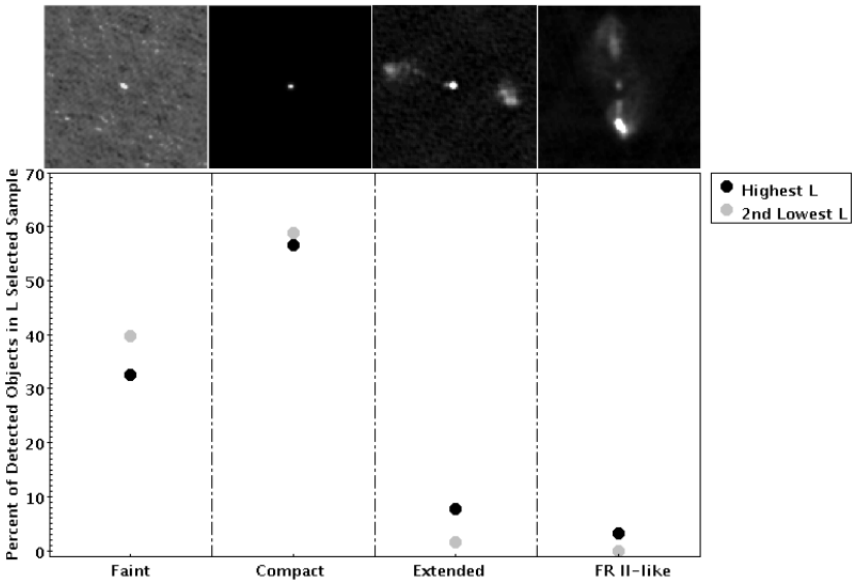

Fig. 7.— Distributions of radio detected quasars for each morphology with example radio images for each classification.

As seen in Figure 7, there are more low luminosity quasars than high luminosity quasars in the faint and compact classifications, whereas there are more high luminosity quasars than low

luminosity quasars in the extended and FRII-like classifications. It makes sense that the high luminosity quasars would have more jets and extended morphologies because jets require a lot of power, meaning that they would probably tend to be brighter as well. This result, as well as the findings from the last section that low optical luminosity quasars typically have more radio emission than high luminosity quasars, suggests that radio emission generally comes from the core of sources rather than extended jets. On the other hand, the lower luminosity sources may be dominated by different radio-generating physics.

Conclusion

Showing that the apparent radio-bimodality was merely due to selection bias will allow future work to include a greater number of potential sources, especially radio intermediate sources. This means investigations of the radio properties of quasars can include a more diverse population, which will potentially fill in some of the missing pieces of the puzzle.

Our results suggest star formation is a probable cause of the increased radio emission seen in red quasars. Our sample size, however, was limited to 10 red quasars and 25 blue quasars. These results would benefit from a larger sample size to increase confidence.

Our finding that low luminosity quasars are more radio loud and are more compact gives us a greater understanding of where radio emission in quasars comes from. Quasars have not changed significantly over the past 13 billion years, and since quasars are generally very old, they allow us to see into the early universe. By understanding the radio properties of quasars, we can gain a better understanding of the evolution of the early universe.

Acknowledgements

We'd like to acknowledge Eilat Glikman and Jonathan Kemp for all of their guidance and help with this research. For this project we used TOPCAT (Taylor, M.B. 2005, Astronomical Data Analysis Software and Systems XIV, 347, 29) to match and analyze tables. We used the SDSS Quasar Catalog fourteenth data release, as well as the Million Quasar Catalog, Version 6.3. We developed a code that uses the python package Selenium to extract 1" cutouts of the deep VLA and FIRST radio images and download the fits files automatically into a chosen directory. The code is publicly available at https://github.com/CheBradley/FitsGrabber. Finally, we'd like to acknowledge the NSF, The Research Corporation, and KNAC for making this research possible.

References

Faucher-Giguère, C.-A., & Quataert, E. 2012, MNRAS, 425, 605
Fliri, J., & Trujillo, I. 2016, MNRAS, 456, 1359
Glikman, E., Simmons, B., Mailly, M., et al. 2015, ApJ, 806, 218
Glikman, E., Lacy, M., LaMassa, S., et al. 2018, ApJ, 861, 37
Ivezić, Ž., Menou, K., Knapp, G. R., et al. 2002, AJ, 124, 2364
Klindt, L., Alexander, D. M., Rosario, D. J., et al. 2019, MNRAS, 1732
Kratzer, R. M., & Richards, G. T. 2015, AJ, 149, 61